Automatika

Journal for Control, Measurement, Electronics, Computing and Communications

ISSN: (Print) (Online) Journal homepage: www.tandfonline.com/journals/taut20

A new approach based on current controlled hybrid power compensator for power quality improvement using time series neural network

Raheni T. D, P. Thirumoorthi & Premalatha K

To cite this article: Raheni T. D, P. Thirumoorthi & Premalatha K (2023) A new approach based on current controlled hybrid power compensator for power quality improvement using time series neural network, Automatika, 64:4, 703-719, DOI: 10.1080/00051144.2023.2203560

To link to this article: https://doi.org/10.1080/00051144.2023.2203560

© 2023 The Author(s). Published by Informa UK Limited, trading as Taylor & Francis Group

Published online: 24 May 2023.

Submit your article to this journal

Article views: 496

View related articles

View Crossmark data

Full Terms & Conditions of access and use can be found at
https://www.tandfonline.com/action/journalInformation?journalCode=taut20

AUTOMATIKA
2023, VOL. 64, NO. 4, 703–719
https://doi.org/10.1080/00051144.2023.2203560

REGULAR PAPER

OPEN ACCESS Check for updates

A new approach based on current controlled hybrid power compensator for power quality improvement using time series neural network

Raheni T. D, P. Thirumoorthi and Premalatha K

Department of Electrical and Electronics Engineering, Kumaraguru College of Technology, Coimbatore, Tamil Nadu, India

ABSTRACT

In this paper, a current controlled-hybrid power compensator (CC-HPC) is presented to reduce the effect of input current harmonics on battery chargers. Passive filters have significant power loss and degrade system frequency due to excessive harmonic attenuation. The proposed system integrates the Higher Order Sliding Mode Controller (HOSMC) with a generalized form of *p*–*q* power theory and a Time Series – Artificial Neural Network (TS-ANN) is used to produce compensating reference current for a three-phase system and generates DC link inductor current. Switching pulses to Current Controlled-Active Power Compensator (CC-APC) switches are generated using a reference compensated signal. The development of CC-HPC and its control approach helps to reduce the overall harmonic distortion of the supply current used in battery chargers are the main contributions of the proposed system. HOSMC is a robust and adaptable controller that tracks reference current without causing chattering is the significant advantage of the proposed method. The control algorithm is designed in MATLAB/SIMULINK software for various load conditions and the experimental setup has been developed for rectified fed RC load using TS-ANN. The filtering process of CC-HPC can maintain the harmonic distortion of supply current within the IEEE 519-2014 standard.

ARTICLE HISTORY
Received 30 May 2022
Accepted 12 April 2023

KEYWORDS
Power quality; PI controller; HOSMC; CC- HPC; time series artificial neural network

1. Introduction

Power quality issues such as voltage and current distortions have been caused by the continuous growth of power electronics converter-based nonlinear loads in domestic and commercial applications. Grid voltage distortion and overheating equipment in distribution network are the main causes of harmonic degradation. An unbalanced three-phase system can seriously distort the power supply. Numerous investigations have shown these voltage distortions vary in duration from a small fraction of a cycle to a few cycles [1]. When the loads are purely resistive, the supply side power factor is unity, while the load current and voltage are ideal in nature. However, if the loads are nonlinear, the voltage and current generated on the supply and load sides are non-sinusoidal, resulting in harmonics in the power system [2]. A nonlinear converter produces an insufficient power factor due to harmonic current injection on the utility side, which in turn reduces system efficiency. Electrical disruption is analysed by current and voltage distortions from the ideal shape in order to detect the disturbances caused by power quality. During a steady state condition, deviations are caused by imbalanced currents, harmonic distortions and voltage profile. The distribution of nonlinear loads over the power grid can cause power quality issues [3]. A distributed system uses inverters to maintain a constant frequency and voltage, even when the load is unbalanced or nonlinear. Various types of nonlinear load create harmonic waveform by producing non-sinusoidal currents on the load side [4]. According to Rajesh Francis et al. [5], the power quality of a system with respect to the deviation of real and reactive power is improved, and it enhances the efficiency of energy storage components in all the systems. The unified power quality conditioner is the most ideal and feasible approach for reducing the power quality issue in modern power systems. The increased usage of dynamic voltage restorer for real–reactive power sharing decreases the demand on UPQC and enhances system efficiency and reliability in all operating scenarios [6]. Active power filter is constructed by interconnecting two separate power converters. This hybrid architecture, on the other hand, is made up of two independent converters that create two separate current sources. The system becomes more complex and time consuming as the number of converters increases [7]. Different types of compensators are used in the research work that include series, shunt and hybrid power compensator. Current harmonics are compensated by shunt power compensator, whereas voltage harmonics are compensated by series power compensator. By using a hybrid power compensator,

CONTACT Raheni T. D raheni.17phd@kct.ac.in Research Scholar, Department of Electrical and Electronics Engineering, Kumaraguru College of Technology, Coimbatore, Tamil Nadu, India

© 2023 The Author(s). Published by Informa UK Limited, trading as Taylor & Francis Group
This is an Open Access article distributed under the terms of the Creative Commons Attribution-NonCommercial License (http://creativecommons.org/licenses/by-nc/4.0/), which permits unrestricted non-commercial use, distribution, and reproduction in any medium, provided the original work is properly cited. The terms on which this article has been published allow the posting of the Accepted Manuscript in a repository by the author(s) or with their consent.

harmonics in both current and voltage are compensated [8]. Based on the previous studies in the literature, it has been determined that there are various issues in the design and control of active power compensator for compensating current harmonics, which are outlined below.

- A passive filter's high impedance compared to load impedance makes it difficult to construct. Passive filters can only be used for a certain amount of compensation, and the methods for compensating reactive power and unbalanced systems are more challenging.
- Harmonic issues can be solved with conventional passive compensators (*L*-*C*). However, these compensators often have a fixed compensation, parallel resonance and overloading issues.
- The active power compensator is expensive when used in isolation and has a high-power rating.
- The majority of traditional control techniques assume perfect supply circumstances with constant loads. However, there may be variations in the input supply, as well as imbalances and distortions in the supply voltage.
- Choosing the appropriate passive elements and active compensator for a given application is essential and the errors obtained in the classical controller can be reduced by implementing intelligent control methods.

As a result, the proposed system uses a hybrid power compensator which compensates imbalanced load. The current controlled-hybrid power compensator is comprised of a passive power compensator (PPC) and a current controlled-active power compensator (CC-APC). In steady state, a conventional proportional integral controller maintains a constant level, but in transient state, the level varies from the initial value. The results of some researchers have been unsatisfactory by using linear control approaches to construct their controllers. The DC inductor current is regulated using a number of advanced signal processing control methods which includes p–q theory, direct testing computation, synchronous reference frame, general integral method, Fourier transform, sliding mode, backstepping algorithm and least mean square (LMS) algorithms. Despite the fact that it is one of those controllers' primary functions is to track the generated reference current accurately and quickly. It is difficult to the rapid change of frequency response of that reference. The attenuation of the switching frequency content would be affected if the reference was followed more precisely. Furthermore, the processing latency of certain current controllers can lead to significant error in the terms of distortion. These critical aspects are also used as performance criteria in this particular scenario [9]. Power components are extracted using the LMS approach, and the weights are estimated using a wiener filter [10]. Model predictive controllers degrade the control problem into steady and transient state problems, which are solved individually to identify harmonics, and power quality issues are improved by using a Kalman filter, as per Narender Reddy [11]. A multi Pulse Width Modulation (PWM) is a periodic signal that is derived from a sequence of discrete real numbers and consists of limited number of Fourier components that are determined by the harmonic content of the signal. The multilevel PWM is a switching signal that contains distortion of harmonics different from those specified. Harmonic distortion is caused by harmonic content in multilevel PWM that is not the part of the prescribed set. As a result, it is better to maintain harmonic distortion to a minimum level for all applications [12].

CC-HPC is a hybrid modulation technique that can be used to generate a sinusoidal current profile with the appropriate phase and magnitude for a wide range of applications. The techniques used to control the compensating reference current have a major impact on the steady and dynamic state performance of the active power compensator. The load current harmonics of the Rectified fed battery charger may fluctuate rapidly and the active power compensator has a rapid-dynamic response to overcome the issues faced by the nonlinearity. As a result, hysteresis controller is used in this study because it is theoretically simple, higher reliability and can be easily implemented in digital controllers [13]. A hysteresis band controller produces a suitable switching signal to CC-HPC and to generate three-phase compensating current at the point of common coupling (PCC) by using fundamental band computation. A fast response to the active power compensator is provided by a carrier-less PWM technique [14]. Sliding mode controller is one among the best methods to reduce harmonic currents in nonlinear systems, although robust controller design is uncertain. The traditional sliding method drives a model by changing the direction of a shape in response to an interrupted signal. When sliding mode algorithm is used, the system states are not examined at a constant rate. The presence of chattering in the sliding mode controller reduces precision, decreases system efficiency, and causes intense heat dissipation in electrical loads. The chattering effect's constraints are reduced by a number of techniques, including dynamic extension, the design of a high gain control algorithm, and the second-order sliding controllers. It is difficult to analyse the stability of bounded time due to uncertainties [15].

Numerous studies have analysed about the reduction of the chattering occurrence, which is discussed in more detail below.

- The inertial delay approach is used to control the unbalanced disruptions present in the multitudinal sliding mode controller. The chattering issue

is solved by the hysteresis function, which ensures that the controller state is transferred to the sliding surface [16]
- The magnitude of chattering phenomenon is reduced to sustainable level by extending the number of phases and establishing a suitable phase difference between each two successive phases. Each phase of a master-slave converter can be supported by numerous consecutively connected "slaves", for a two-phase converter, so that the entire phase difference equals the specific value [17].

The hysteresis band's breaking points are improved via the nonlinear sliding approach. Consequently, switching losses are reduced and ripples in the grid current are minimized [18]. The proposed methodology uses a higher-order sliding mode controller along with a generalized form of p–q theory to prevent the undesirable oscillation (chattering) that results in high switching frequency. To calculate the CC-HPC state space model, the uncertainties of system parameters must initially be taken into consideration. An inductor is connected parallel to the utility grid at the point of common coupling in which the CC-HPC compensates the source current harmonics. The large number of active harmonic compensators, especially when tuning proportional integral controllers, requires a complex numerical model. Even though the PI controller is effective for steady and transient state conditions, its gain values have a significant overshoot, which delays the response of the system. It is difficult to develop a computational model using conventional methods because of nonlinear parameter changes. This problem can be solved using artificial intelligence (AI) techniques such as neural networks, multi-modal optimization algorithms, fuzzy logic and emotional controllers. It is possible for machines to simulate human-like intelligence through these methods. Moreover, training with evolutionary control algorithms requires more time due to the prolonged computational period. According to Keyhan Kobravi [19], the search process in multi-modal optimization technique has less intense than sequential and arbitrary search but it is less complicated than iterative process. The accuracy of the final outcome is adjusted by optimization algorithm. The proposed system is implemented with time series – artificial neural network-based HOSMC. The model is controlled by a biological neural network.

Neural network provides reference current for the current controlled – hybrid power compensator because of its parallel computation and learning process. The error is minimized by training the weight of each input neuron and compensating current reference is generated with minimum oscillation. The weight is updated by using gradient descent method [20]. In contrast to fine-tuning the PI controller, the neural controller is highly robust in improving the input and system parameters. Furthermore, the proposed HOSMC helps to minimize the chattering to the greatest extent possible. The contributions of the proposed systems are given below:

- The source current harmonics are reduced by a proposed current controlled – hybrid power compensator.
- The proportional integral tuned HOSMC with the generalized P–Q theory is designed for time-varying sliding surfaces.
- The proposed method is estimated for proportional integral tuned higher order sliding controllers.
- Time series – artificial neural network algorithm is implemented and analysed with PI-tuned HOSMC.
- Harmonic analysis of input current in the consumer end is reduced to IEEE-519-2014 standard ($< 5\%$).
- The experimental setup for rectified fed RC load has been developed using neural algorithm-based HOSMC.

2. Design of higher order sliding mode controller for harmonic current compensation

Higher order sliding mode controller encompasses variable time states with intermittent feedback process that frequently switch from one linear structure to other structure in accordance with the original state. Figure 1 depicts a power circuit without harmonic compensator and a PI controller-based HOSMC with time series neural algorithm. The power circuit is formed by connecting a three-phase supply to rectifier-fed battery charger. It is essential to reduce the unwanted harmonic distortion in the input side. Input voltage, load current, DC link current and I_{dc_Ref} are inputs for a proportional-integral controller tuned HOSMC. The sliding mode parameters S_1, S_2, S_3 and S_4 are analytically determined from HOSMC and the three-phase reference current is produced from the generalized form of p–q theory. Similarly, the generated current reference is delivered to the hysteresis band control. CC-APC uses the switching PWM signals produced by the hysteresis band to produce the compensated filter current. The measured CC-HPC currents (I_{F-abc}) are compared with compensating reference currents (I_{C-abc}) through comparator block. The current error signal is determined by each comparator and fed as an input to the relay with a reduced hysteresis band. This relay maintains the switching functions of the IGBT switches in the three inverter legs (S_1, S_3, S_5) such that the filter current maintains within the specified hysteresis band. Switching is made to reduce the filter current when the error signal exceeds the upper bound, and vice versa. The proposed hybrid compensator with HOSMC is shown in Figure 1.

The proposed compensator produce harmonic – less current on the source side by cancelling the battery

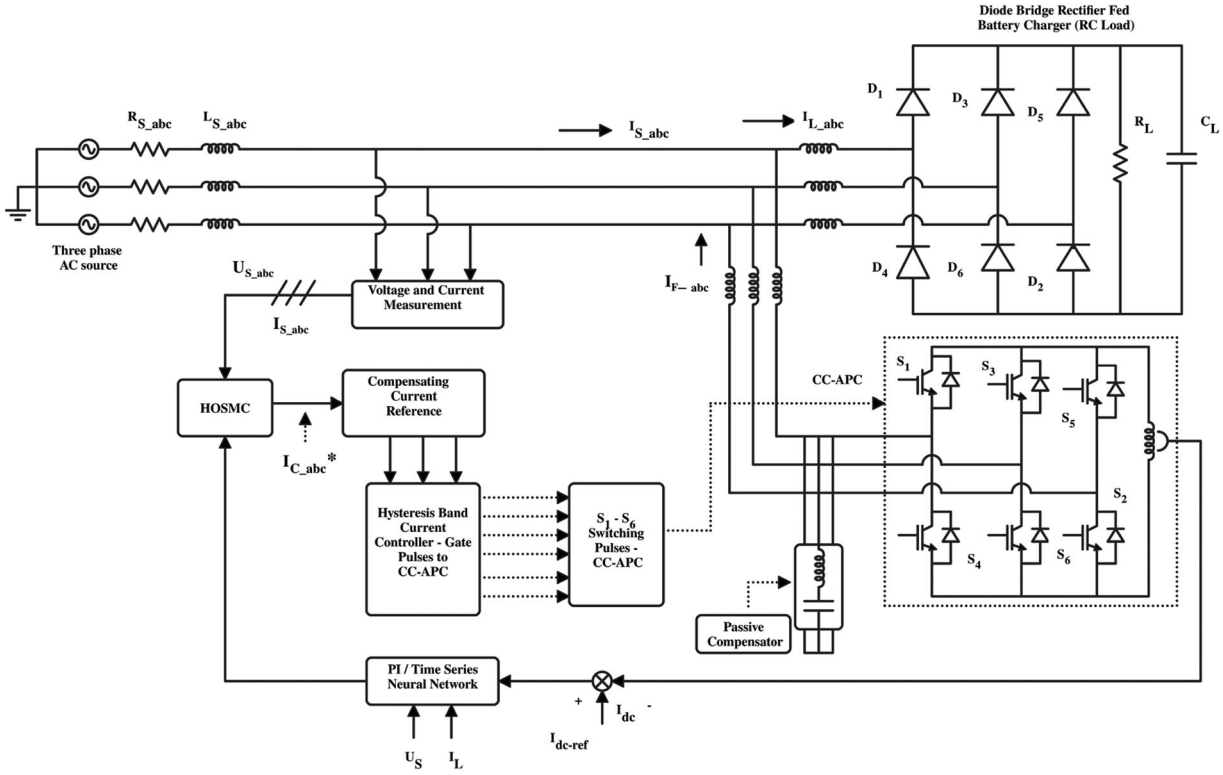

Figure 1. Proposed hybrid compensator with HOSMC.

charger load currents and filter currents at the PCC. This system has been designed to prevent the network's chattering affect for the section of relative degree two. The designed controller effectively suppresses the chattering issue and improves the variation of parameters occurring in the system.

2.1. Modelling of HOSMC

Higher order sliding mode controller consists of current and voltage control loop. The mathematical model of PI-tuned HOSMC is discussed in this section.

Derivative function for input voltage and load current is as follows:

$$\frac{dU_S}{dt} = \left[\frac{1}{C_F} - \frac{1}{C_F}\right]\begin{bmatrix} I_s \\ I_L \end{bmatrix} \tag{1}$$

$$L_S\left[\frac{dI_L}{dt}\right] = \left[\frac{1}{L_F} - \frac{1}{L_F}\right]\begin{bmatrix} U_S \\ U_L \end{bmatrix} \tag{2}$$

Where L_S refers for the load current state equations.

$$L_S = \begin{pmatrix} 1 & -1 & 0 \\ 0 & 1 & -1 \\ -1 & 0 & 1 \end{pmatrix}$$

U_S is converter source voltage and is represented as $[U_S] = [U_{Sa}, U_{Sb}, U_{Sc}]^{\mathrm{T}}$. I_L is the converter load current and is denoted by $[I_L] = [I_{La}, I_{Lb}, I_{Lc}]^{\mathrm{T}}$. U_L represents the load voltage.

Three phase reference a-b-c frame from Equations (1) and (2) are converted to synchronous direct and quadrature axis frame (d–q).

$$\frac{dU_{Sd}}{dt} = \omega U_{Sq} - \frac{1}{C_F}I_{Ld} + \frac{1}{C_F}I_{Sd} \tag{3}$$

$$\frac{dU_{Sq}}{dt} = -\omega U_{Sd} - \frac{1}{C_F}I_{Lq} + \frac{1}{C_F}I_{Sq} \tag{4}$$

$$\frac{dI_{Ld}}{dt} = -\frac{1}{L_F}U_{Sd} + \omega I_{Lq} + \frac{1}{L_F}U_{Ld} \tag{5}$$

$$\frac{dI_{Lq}}{dt} = -\frac{1}{L_F}U_{Sq} - \omega I_{Ld} + \frac{1}{L_F}U_{Lq} \tag{6}$$

where $\omega = 2\Pi f$ refers to the angular frequency. The input current and voltage of the d–q axis are denoted by I_{Sd}, I_{Sq} and U_{Sd}, U_{Sq}. Similarly, the load current and voltage of d–q axis are represented as I_{Ld}, I_{Lq} and U_{Ld}, U_{Lq}. It is assumed that the capacitor and inductor's active harmonic compensators are C_F as Y_1 and L_F as Y_2, respectively. Because some parameters are difficult to precisely determine, they can be considered as variable parameters.

Variable parameters of the proposed system are determined as

$$Y_1 = Y_{1m} + \Delta Y_1$$

$$Y_2 = Y_{2m} + \Delta Y_2$$

where Y_{1m} and Y_{2m} are represented as nominal values and Δ_{Y1}, Δ_{Y2} are denoted as parameter uncertainties. Equations (3)–(6) are simplified to:

$$(Y_{1m} + \Delta Y_1)\frac{dU_{Sd}}{dt} = \omega(Y_{1m} + \Delta Y_1)U_{Sq} - I_{Ld} + I_{Sd} \tag{7}$$

$$(Y_{1m}+\Delta Y_1)\frac{dU_{Sq}}{dt} = -\omega(Y_{1m}+\Delta Y_1)U_{Sd} - I_{Lq} + I_{Sq} \quad (8)$$

$$(Y_{2m}+\Delta Y_2)\frac{dI_{Ld}}{dt} = \omega(Y_{2m}+\Delta Y_2)I_{Lq} - U_{Sd} + U_{Ld} \quad (9)$$

$$(Y_{2m}+\Delta Y_2)\frac{dI_{Lq}}{dt} = -\omega(Y_{2m}+\Delta Y_2)I_{Ld} - U_{Sq} + U_{Lq} \quad (10)$$

From Equation (7) to Equation (10), the mathematical representation of the inverter side can be stated as follows:

$$\frac{dU_{Sd}}{dt} = -\frac{I_{Ld}}{Y_{1m}} + \omega U_{Sq} + \frac{\Delta Y_1}{Y_{1m}}\left(\omega U_{Sq} - \frac{d}{dt}U_{Sd}\right) + \frac{I_{Sd}}{Y_{1m}} \quad (11)$$

$$\frac{dU_{Sq}}{dt} = -\frac{I_{Lq}}{Y_{1m}} - \omega U_{Sd} - \frac{\Delta Y_1}{Y_{1m}}\left(-\omega U_{Sd} - \frac{d}{dt}U_{Sq}\right) + \frac{I_{Sq}}{Y_{1m}} \quad (12)$$

$$\frac{dI_{Ld}}{dt} = -\frac{U_{Sd}}{Y_{2m}} + \omega I_{Lq} + \frac{U_{Ld}}{Y_{2m}} + \frac{\Delta Y_2}{Y_{2m}}\left(\omega I_{Lq} - \frac{d}{dt}I_{Ld}\right) \quad (13)$$

$$\frac{dI_{Lq}}{dt} = -\frac{U_{Sq}}{Y_{2m}} - \omega I_{Ld} + \frac{U_{Lq}}{Y_{2m}} - \frac{\Delta Y_2}{Y_{2m}}\left(\omega I_{Ld} + \frac{d}{dt}I_{Lq}\right) \quad (14)$$

N_1, N_2, N_3 and N_4 represent the nominal model function, ΔN_1, ΔN_2, ΔN_3 and ΔN_4 denote the uncertain function model and input control variables are denoted by h_1, h_2, h_3 and h_4.

$$N_1 = \omega U_{Sq}; N_2 = -\omega U_{Sd}; N_3 = -\frac{U_{Sd}}{Y_{2m}} + \omega I_{Lq};$$

$$N_4 = -\frac{U_{Sq}}{Y_{2m}} - \omega I_{Ld};$$

$$\Delta N_1 = \frac{\Delta Y_1}{Y_{1m}}\left(\omega U_{Sq} - \frac{d}{dt}U_{sd}\right) + \frac{I_{Sd}}{Y_{2m}}$$

$$\Delta N_2 = -\frac{\Delta Y_1}{Y_{1m}}\left(-\omega U_{Sd} - \frac{d}{dt}U_{sq}\right) + \frac{I_{Sq}}{Y_{2m}}$$

$$\Delta N_3 = \frac{\Delta Y_2}{Y_{2m}}\left(\omega I_{Lq} - \frac{d}{dt}I_{Ld}\right);$$

$$\Delta N_4 = -\frac{\Delta Y_2}{Y_{2m}}\left(\omega I_{Ld} + \frac{d}{dt}I_{Lq}\right);$$

$$h_1 = \frac{I_{Ld}}{Y_{1m}}; h_2 = -\frac{I_{Lq}}{Y_{1m}}; h_3 = \frac{U_{Ld}}{Y_{2m}}; h_4 = \frac{U_{Lq}}{Y_{2m}}$$

With 25% uncertain parameters, the system performed best, hence 0.25 is chosen for $Y_1 = 0.25\ Y_{1m}$ and $Y_2 = 0.25\ Y_{2m}$, where $Y_{1\mathrm{m}}$ and Y_{2m} are the corresponding gain values. The current and voltage controller are incorporated to the equations from (11) to (14) through Equations (15)–(18).

$$\frac{dI_{Ld}}{dt} = N_1 + \Delta N_1 + h_1 \quad (15)$$

$$\frac{dI_{Lq}}{dt} = N_2 + \Delta N_2 + h_2 \quad (16)$$

$$\frac{dU_{Sd}}{dt} = N_3 + \Delta N_3 + h_3 \quad (17)$$

$$\frac{dU_{Sq}}{dt} = N_4 + \Delta N_4 + h_4 \quad (18)$$

The calculation of sliding variable for load current is given below:

$$S_1 = I_{Ld} - I_{Ld_Ref} \quad (19)$$

$$S_2 = I_{Lq} - I_{Lq_Ref} \quad (20)$$

Whereas I_{Ld_Ref} and I_{Lq_Ref} are represented as load current reference values and it is assumed as,

$$-I_{Ld_Ref} = r_1; -I_{Lq_Ref} = r_2$$

Derivative function $(\dot{S}_1, \dot{S}_2)$ is obtained by incorporating Equations (19) and (20) in Equations (15) and (16).

$$\dot{S}_1 = -I_{Ld_Ref} + N_1 + \Delta N_1 + r_1 \quad (21)$$

$$\dot{S}_2 = -I_{Lq_Ref} + N_2 + \Delta N_2 + r_2 \quad (22)$$

The calculation of sliding mode variables for input voltage is determined by,

$$S_3 = U_{Sd} - U_{Sd_Ref} \quad (23)$$

$$S_4 = U_{Sq} - U_{Sq_Ref} \quad (24)$$

Whereas U_{Sd_Ref} and U_{Sq_Ref} are denoted as input source voltage references and by defining $-U_{Sd_Ref} = r_3$ and $-U_{Sq_Ref} = r_4$.

The time derivative function of the sliding mode variables for Equations (23) and (24) is related with Equations (17) and (18) we get,

$$\dot{S}_3 = -U_{Sd_Ref} + N_3 + \Delta N_3 + r_3 \quad (25)$$

$$\dot{S}_4 = -U_{Sq_Ref} + N_4 + \Delta N_4 + r_4 \quad (26)$$

$\dot{S}_1$ and $\dot{S}_2$ are the time derivatives of control variable for the current control loop, which is stated in two phases (d–q). The compensating currents in d–q axis are given below:

$$I_{Cd} = \frac{-1}{\left(\dot{S}_1^2 + \dot{S}_2^2\right).\left(\left(P_r.\dot{S}_1\right) + \left(Q_i.\dot{S}_2\right)\right)} \quad (27)$$

$$I_{Cq} = \frac{-1}{\left(\dot{S}_1^2 + \dot{S}_2^2\right).\left(\left(P_r.\dot{S}_2\right) - \left(Q_i.\dot{S}_1\right)\right)} \quad (28)$$

The d–q axis from the generalized form of p–q theory is used for power calculation.

$$\begin{aligned}
&\text{Voltage Vector}, u = U_{Sd} + jU_{Sq}\\
&\text{Current Vector}, i = I_{Ld} + jI_{Lq}\\
&\text{Power} = u * i\\
&= (U_{Sd} + jU_{Sq}) * (I_{Ld} + jI_{Lq})\\
&= U_{Sd}I_{Ld} + j(U_{Sq}I_{Ld}) + j(U_{Sd}I_{Lq}) - U_{Sq}I_{Lq}\\
&= (U_{Sd}I_{Ld} - U_{Sq}I_{Lq}) + j(U_{Sd}I_{Lq} + U_{Sq}I_{Ld})\\
&= P_r + jQ_i
\end{aligned}$$

P_r and Q_i are real (active) power and imaginary (reactive) power determined by generalized form of p–q theory.

$$P_r = U_{sd}i_{Ld} - U_{sq}i_{Lq} \tag{29}$$

$$Q_i = U_{sd}i_{Lq} + U_{sq}i_{Ld} \tag{30}$$

In a similar manner, the equations for the compensated voltage in the d–q frame are

$$U_{Cd} = \frac{-1}{\left(\dot{S}_3^2 + \dot{S}_4^2\right).\left(\left(P_r.\dot{S}_3\right) + \left(Q_i.\dot{S}_4\right)\right)} \tag{31}$$

$$U_{Cq} = \frac{-1}{\left(\dot{S}_3^2 + \dot{S}_4^2\right).\left(\left(P_r.\dot{S}_4\right) - \left(Q_i.\dot{S}_3\right)\right)} \tag{32}$$

$\dot{S}_3$ and $\dot{S}_4$ are the derivative function of sliding parameters for the voltage control loop. The three-phase I_{a-b-c} current is generated by converting the two-phase compensating currents from d–q frame, respectively.

$$I_{Ca} = \sqrt{2/3}.I_{Cd} \tag{33}$$

$$I_{Cb} = \sqrt{2/3}.\left[(-0.5.I_{Cd}) + \sqrt{3/2}.I_{Cq}\right] \tag{34}$$

$$I_{Cc} = \sqrt{2/3}.\left[(-0.5.I_{Cd}) - \left(\sqrt{3/2}.I_{Cq}\right)\right] \tag{35}$$

By using PI-tuned HOSMC and a generalized form of p–q theory, three phase reference compensating current is produced. Total harmonic distortion (THD) of the input current with proposed PI-tuned HOSMC is 4.63% (Load 1) and 3.21% (Load 2). The neural network-tuned HOSMC further enhances the performance of input current's THD. The data from the conventional PI-tuned HOSMC delivers the input reference signal to the time series neural network controller.

3. Time series – artificial neural network

During the learning process, the network is highly refined for nonlinear mapping and harmonic compensation with load balancing is achieved. Operation of training dataset is obtained by PI-tuned HOSMC. The network connects a set of numeric inputs and outputs to a dataset. Through the regression process, the network gets trained and error is minimized between the actual output and the essential target data [21] as per the below Equation,

$$e = Y_{\text{actual}} - Y_{\text{target}} \tag{36}$$

The learning rule changes the internal weight of the neuron, which represents the data set to reduce the error function. The samples of DC link and reference DC link current obtained from PI controller are chosen for training the network. If the network satisfies the validation process, time series Simulink model is generated. The analysis of the neural network is continued until the data satisfy with good results. The results are compared with classical PI-tuned HOSMC.

The TS-ANN design is shown in Figure 2 which has eight inputs: three phase-source voltage (U_{Sa}, U_{Sb}, U_{Sc}), three phase-load current (I_{La}, I_{Lb}, I_{Lc}) and I_{DC} and $I_{\text{DC_Ref}}$. The outputs of the TS-ANN with 30 hidden neurons are chosen to generate compensating current reference (I_{Ca}, I_{Cb} and I_{Cc}).

4. Results and discussions

The system is developed with PI-tuned HOSMC and TS-ANN that operates under different load circumstances. The control parameters of the proposed work are depicted in Table 1.

Table 1. Specifications of the control parameters.

Parameters	Symbol	Values
Source voltage	V_S	440 V
Supply frequency	F	50 Hz
Phase	Ph	Three
Rectified fed RC Load	R & C	$R_1 = 250\ \Omega; C_1 = 10\ \mu F$ $R_2 = 75\ \Omega; C_2 = 100\ \mu F$
Proportional controller gain	K_P	5.35
Integral controller gain	K_i	27.50
Input resistance	R_S	2.75 Ω
Input inductance	L_S	0.25 mH

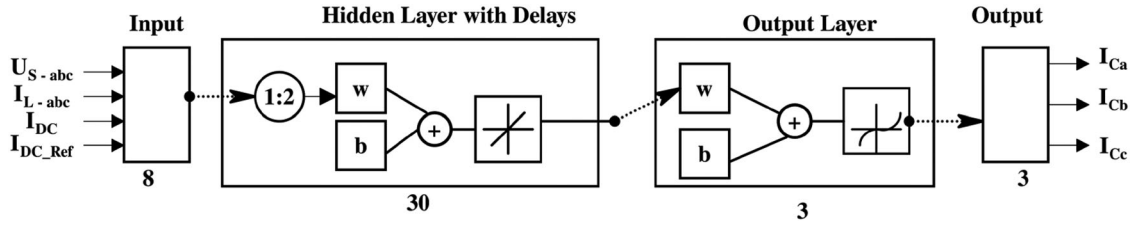

Figure 2. Design of proposed time series – artificial neural network.

4.1. Current harmonics – before compensation

Three phase diode bridge rectifiers fed RC nonlinear load produces distorted current in input side. The distorted current produced for the two varying RC loads requires compensation as total harmonic distortion of input source current is not within IEEE standards. Figure 3 explains the input current profile of battery charger without filter for two different loads. The time period from 0.4 Sec to 0.5 Sec the amplitude of source current is 1.85 A and 0.5 Sec to 0.6 Sec the amplitude of source current is 3.6 A.

The Fourier analysis of two different loads is shown in Figures 4 and 5. The overall harmonic distortion of source current for load 1 is 30.50%, whereas it is 23.34% for load 2. The harmonic distortion produced by battery charger is reduced by implementing PI and time series neural algorithm.

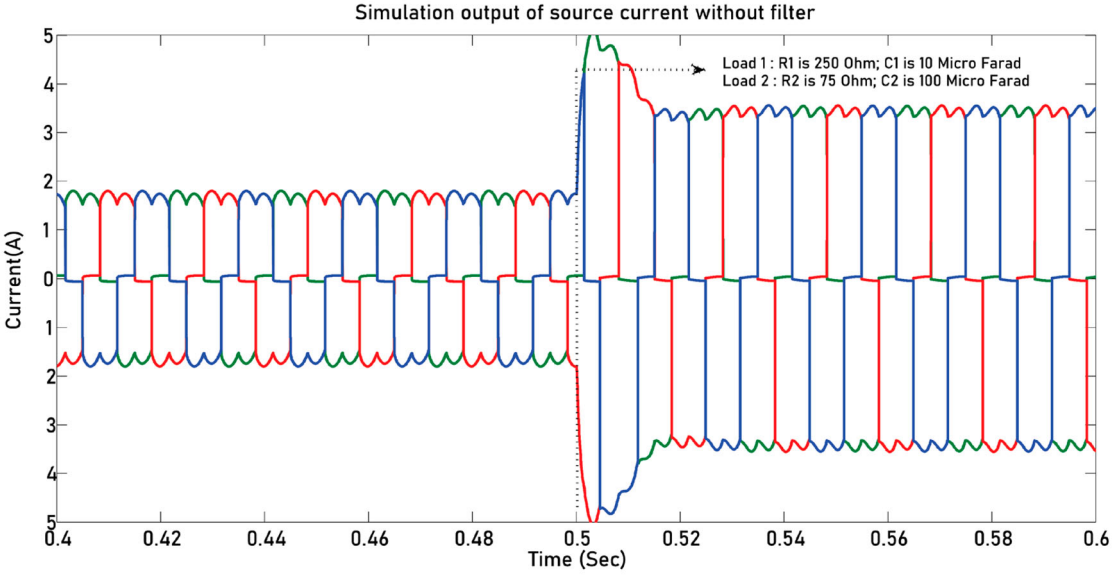

Figure 3. Source current waveform of battery charger – before compensation.

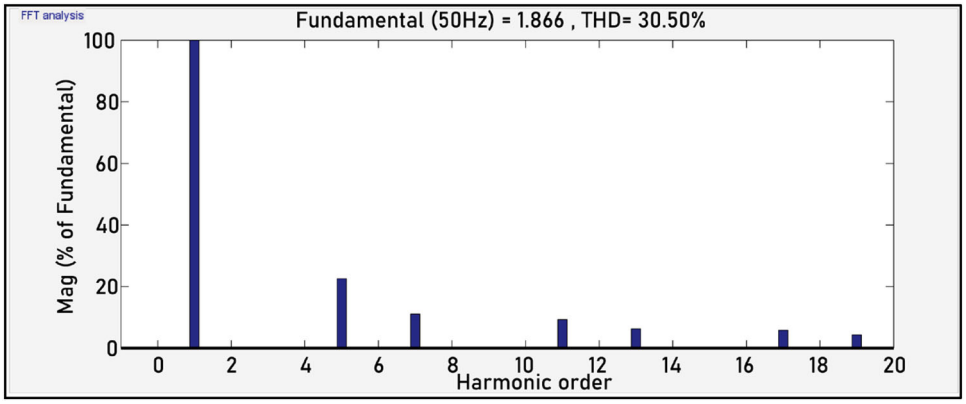

Figure 4. Fourier analysis of input current before compensation – Load 1.

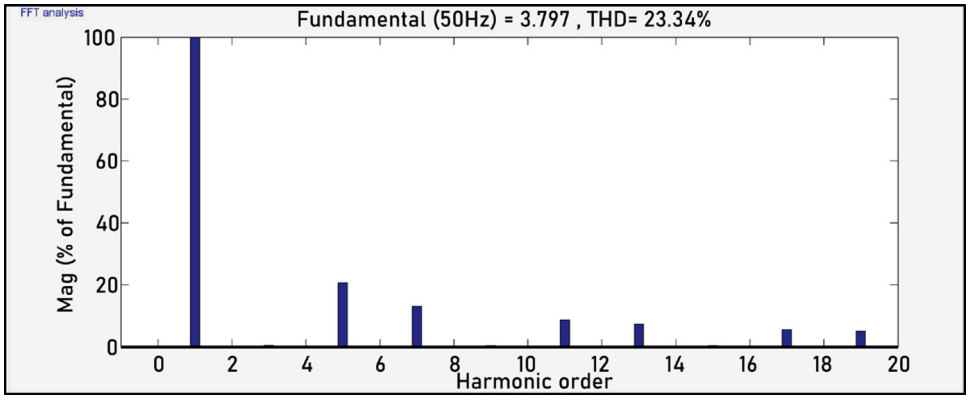

Figure 5. Fourier analysis of input current of Load 2 before compensation.

4.2. Current harmonics after compensation – PI-tuned HOSMC

Simulink model of PI-tuned HOSMC is shown in Figure 6 which consists of control circuit, hysteresis band current controller and the compensator circuit.

It was observed that the harmonic disturbance of the input current is reduced by implementing PI-tuned HOSMC using MATLAB Simulink. In Figure 7, the results of Proportional Integral tuned HOSMC are presented. In this figure, (a) V_s determines the input voltage with amplitude of 600 V, (b) I_L depicts the load current for two distinct loads having distorted outcomes, (c) I_f represents the compensated filter current, (d) the input source current (I_S) produced by battery charger is reduced to IEEE 519-2014 standard, in which the harmonics are reduced by implementing PI-tuned HOSMC and (e) I_{dc} represents the DC inductor current.

The supply current becomes sinusoidal and the distortion reduces from 30.50% to 4.63% (Load 1) and from 23.34% to 3.21% (Load 2) as per IEEE standard. Figures 8 and 9 illustrate the Fourier analysis of the PI-tuned HOSMC (source current) for the load 1 at 0.4–0.5 Sec and the load 2 at time 0.5–0.6 Sec.

4.3. Current harmonics after compensation – time series neural network algorithm

With 66,771 PI controller samples are used to train the neural network and 30 hidden neurons are chosen. The network's execution is calculated with 473 iterations using mean square error. It is necessary to use primary weights so that the network can converge rapidly with a minimum amount of error.

Training set continues when the error for the training data set decreases. The network is designed to retain the training set to a specific level, when the error performance is increased. During this stage, the set of training data is denoted as T, set of weights that need to be

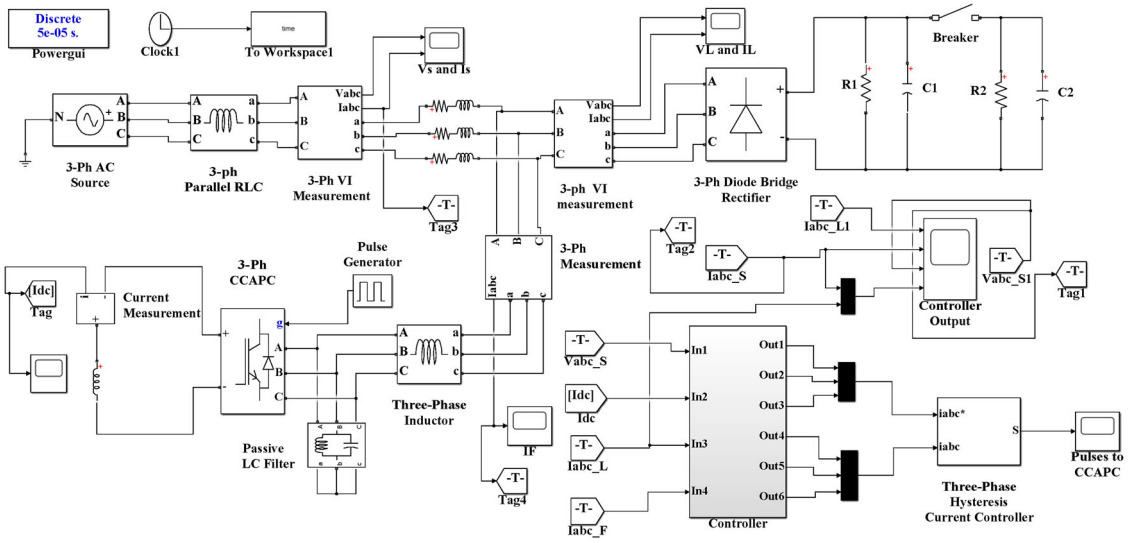

Figure 6. Simulink model of CC-HPC.

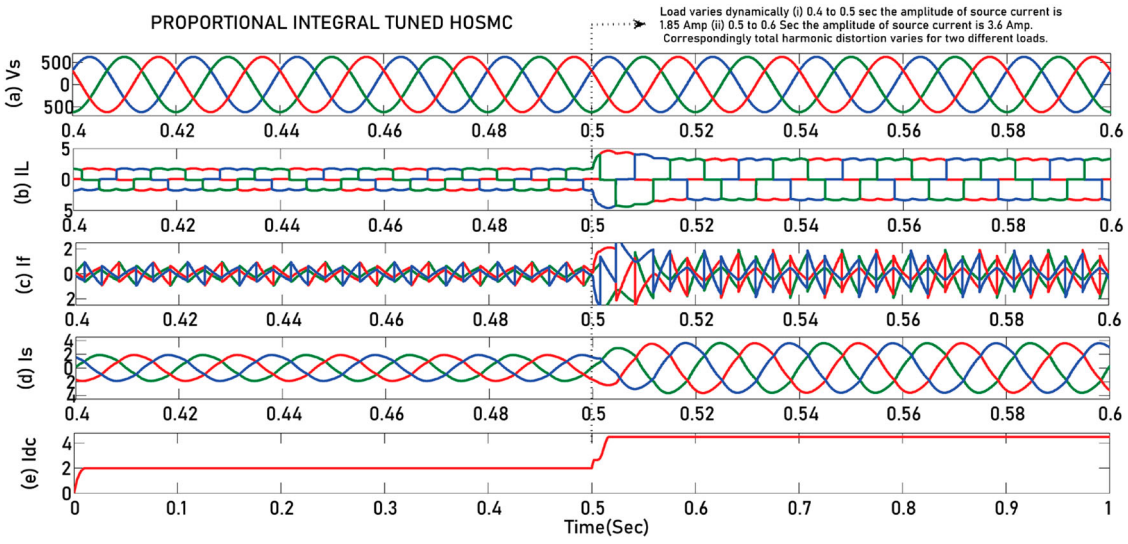

Figure 7. Results of proportional integral tuned HOSMC. (a) Input voltage, U_S; (b) Load current, I_L; (c) Compensating filter current, I_F; (d) Supply current, I_S; (e) DC link inductor current, I_{DC}.

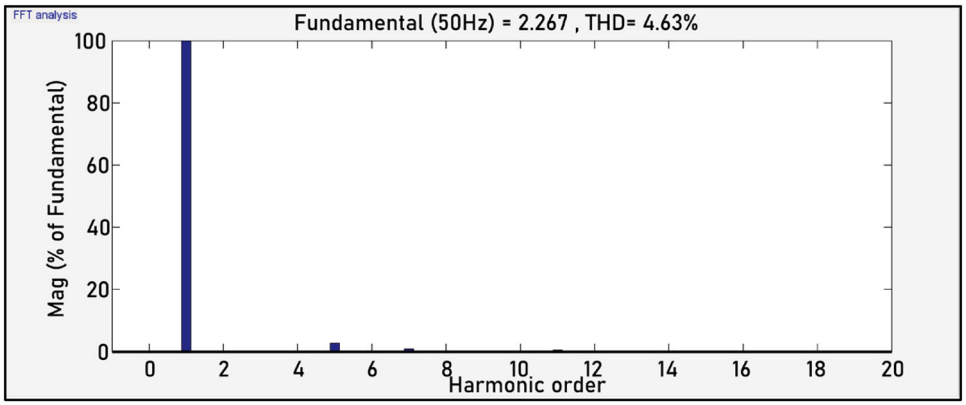

Figure 8. Fourier analysis of source current with PI controller – Load 1.

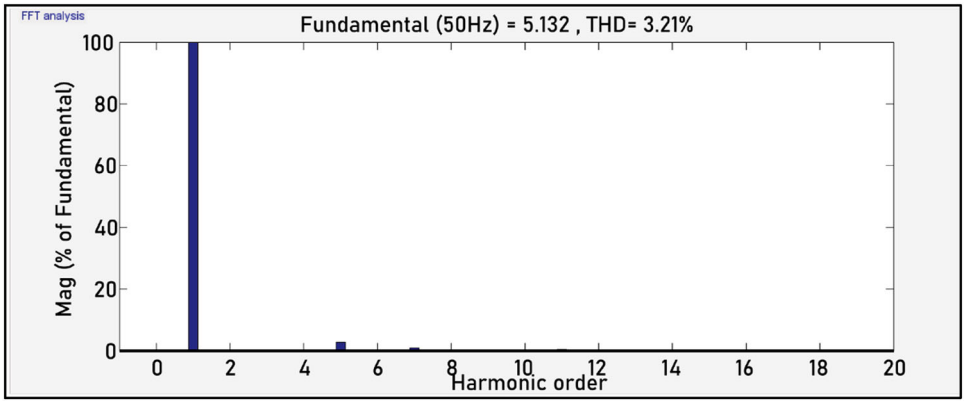

Figure 9. Fourier analysis of source current of load 2 with PI controller.

trained is W and the predicted accuracy is denoted as A. These three terms are connected by the equation,

$$\frac{\text{Weight}}{\text{Training}} = \text{Accuracy} \tag{37}$$

Training process of TS-ANN is shown in Figure 10.

The 66,771 PI controller samples are divided into three divisions at random. A total of 70% of the samples are used in the training segment, which includes 10,016 samples. The network gets adjusted during the training process based on its error mapping. The validation and testing steps require 15% of the total samples, respectively. Figure 11 shows the validation and test data of the proposed system.

Testing performance of the proposed system is shown in Figure 12. The best validation result is

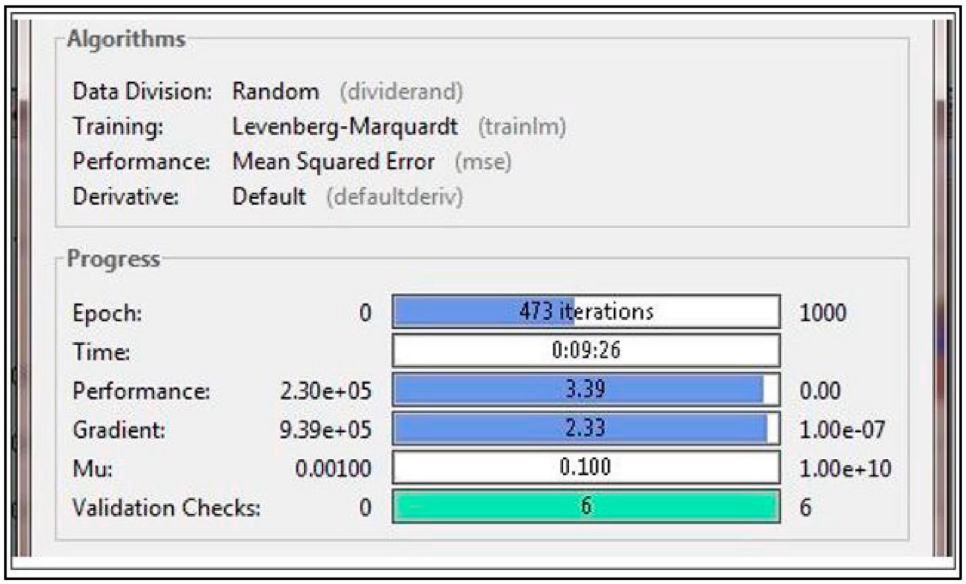

Figure 10. Training process of time series – artificial neural network.

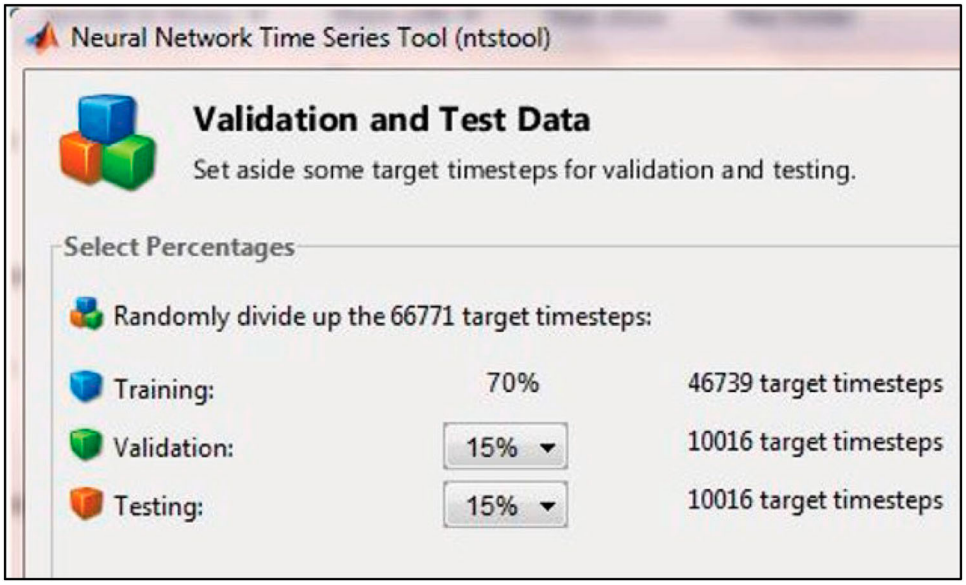

Figure 11. Proposed validation and test data of TS-ANN.

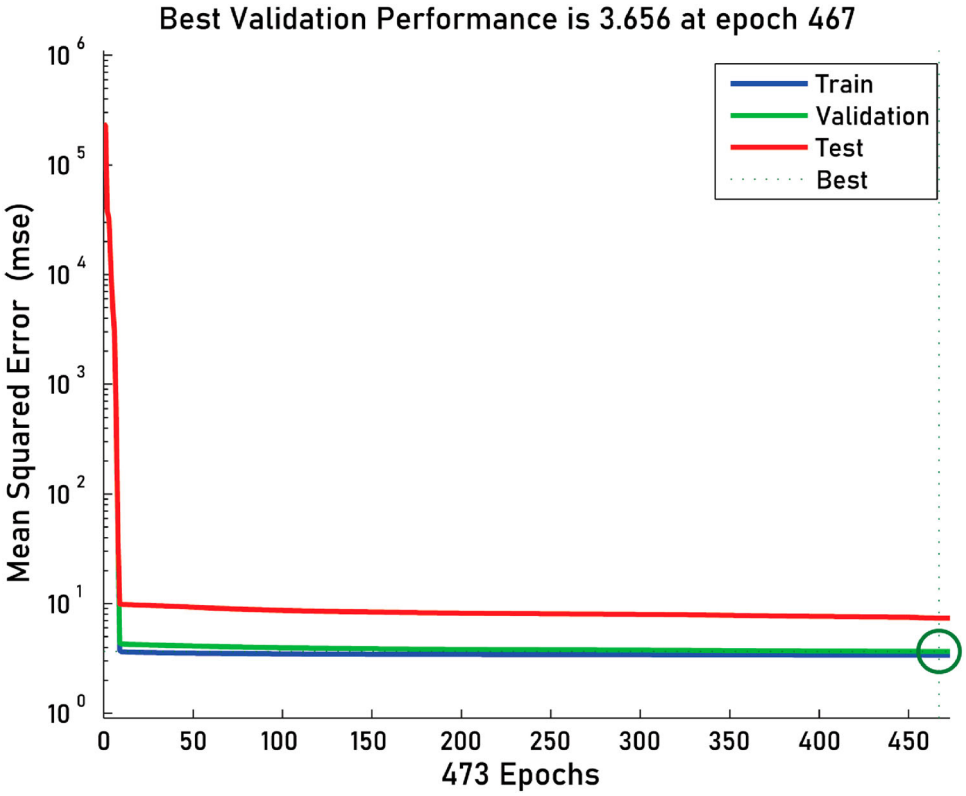

Figure 12. Validation performance of TS-ANN.

attained at the 467 iterations out of 473 iterations. According to observations, the system's performance varies depending on the input data and hidden units.

The network forecasts an output variable as a function of the inputs using a regression procedure. Proposed regression analysis is shown in Figure 13.

Response curve of the proposed system is shown in Figure 14.

The results of TS-ANN are shown in Figure 15 in which the harmonic current produced in supply side is reduced to IEEE 519-2014 standard (< 5% THD for source current). The %THD of input supply current is reduced by utilizing neural controller (Figure 15) as compared to PI controller (Figure 7). I_{dc} current in TS-ANN is significantly improved and stabilized at the amplitude of 3.6 A.

Fourier analysis of input source current for the two different loads is shown in Figure 16 and 17.

The proposed TS-ANN is developed for battery charger applications has achieved the best results by reducing the harmonic distortion of supply current. According to the results of the harmonic spectrum

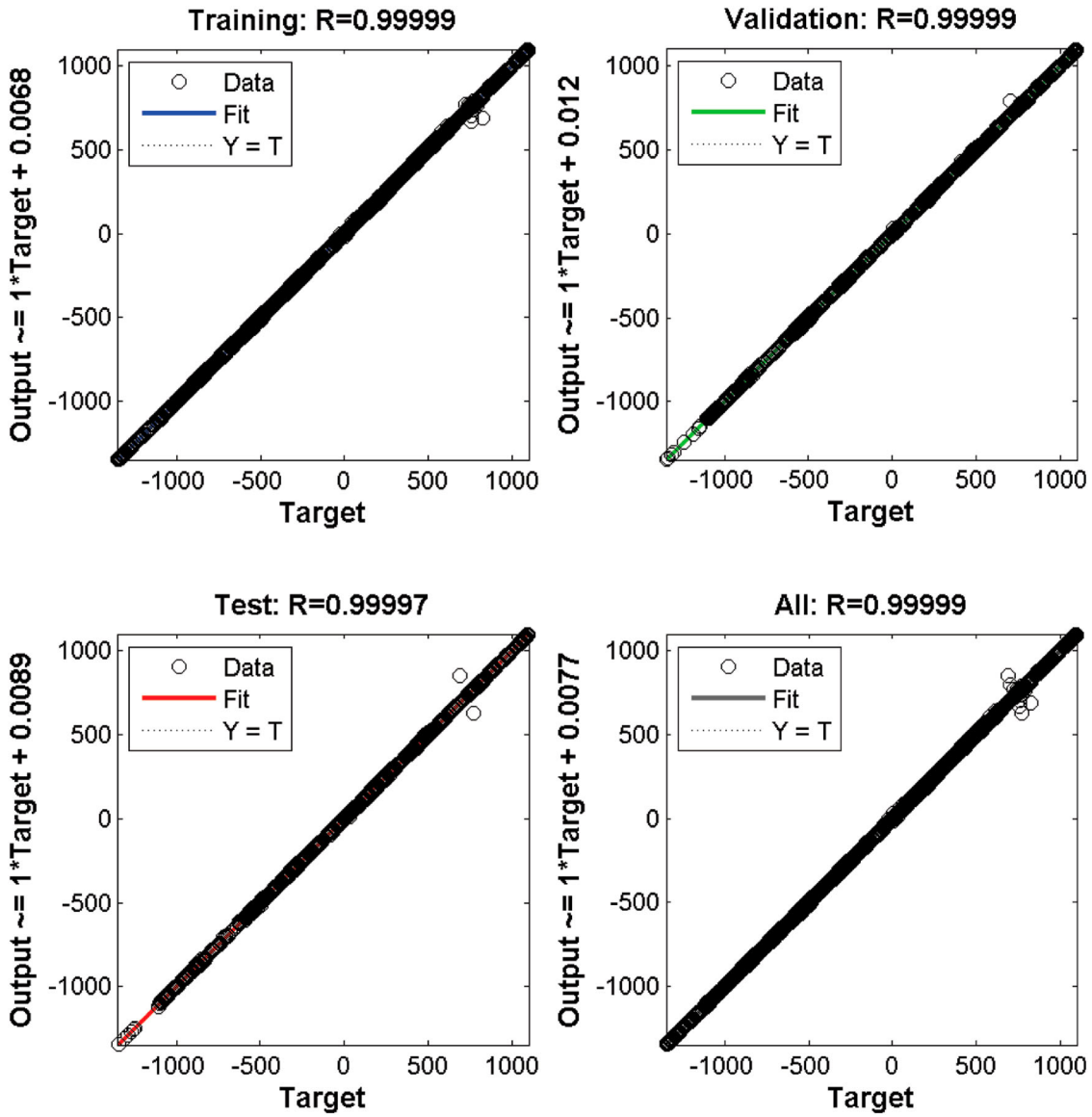

Figure 13. Regression plot analysis of TS-ANN.

analysis, the majority of the primary harmonic components are reduced when the TS-ANN controller is used in battery charger applications to improve power quality disturbances.

4.4. Experimental results

Experimental setup of CC-HPC is depicted in Figure 18. It consists of three phase – three leg current source inverter and IGBT power module (PEC16DSM01) through a FPGA Spartan 3A with DSP. Three phase supply of 100 V, with frequency of 50 Hz and source inductance of 0.25 mH is connected to rectified fed RC load ($R = 30\,\Omega$ and $C = 100\,\mu F$). The CC-HPC of inductor current is 15 mH. Hall sensors are used to monitor voltage (LV 25-P) and current (LTS 25-NP). The sensing circuits are developed and the measured voltages and currents are delivered to DSP by analogue to digital converter. In addition to the DSP, a power quality analyser and a simulation instrument (DSO) are used to record the results for steady-state and dynamic loads.

This research examines the three-phase rectified fed RC load since the rectifier serves as the primary converter for variable-speed drives and power supply units. The controller receives input from U_s, I_s, I_{DC}, I_L, I_F and rectifier obtains power from an auto and step-down transformer. The intelligent power module is a bridge-type inverter consists of IGBT along with driver and protection circuits. A high-frequency ferrite core inductor is used to connect it to the PCC. The FPGA controller is used to produce compensating reference of three phase current and DC link inductor current regulation. Experimental results are shown in Figure 19.

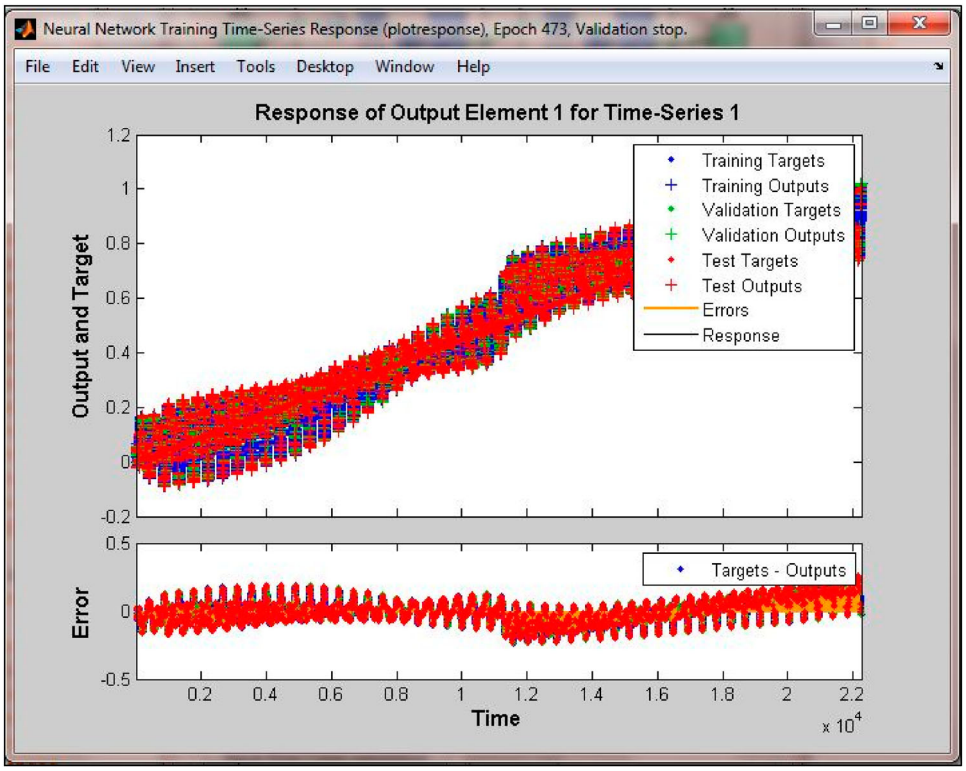

Figure 14. Proposed time series response of neural network.

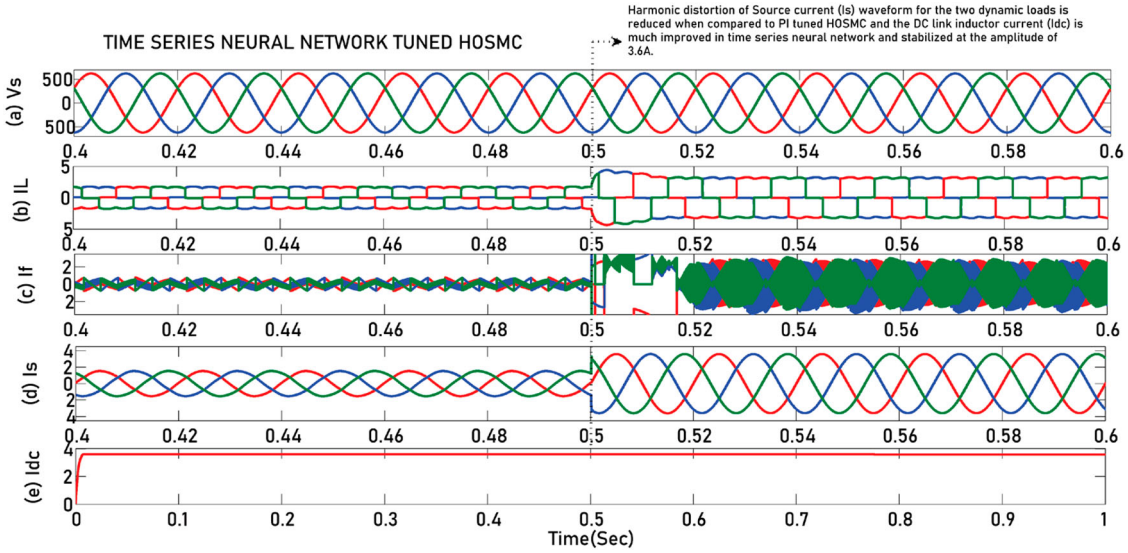

Figure 15. Results of time series – artificial neural network tuned HOSMC (a) Supply voltage, U_S; (b) Battery charger current, I_L; (c) Compensating current, I_F; (d) Source current, I_S; (e) DC inductor current, I_{DC}.

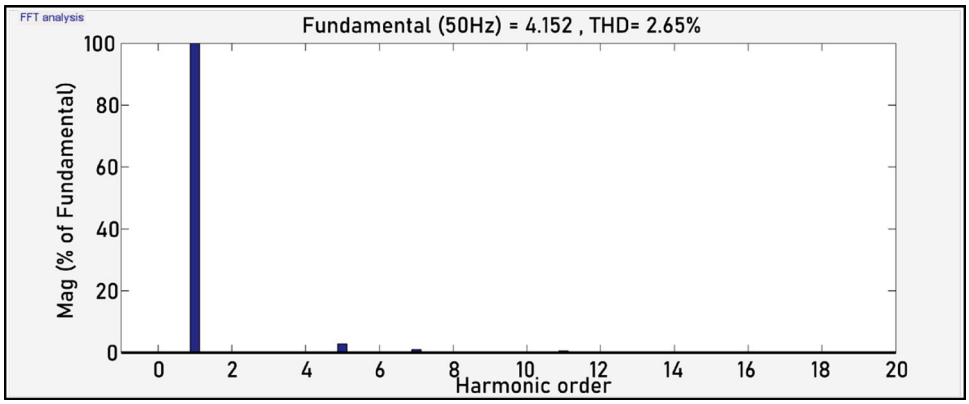

Figure 16. Fourier analysis of source current with time series neural network – Load 1.

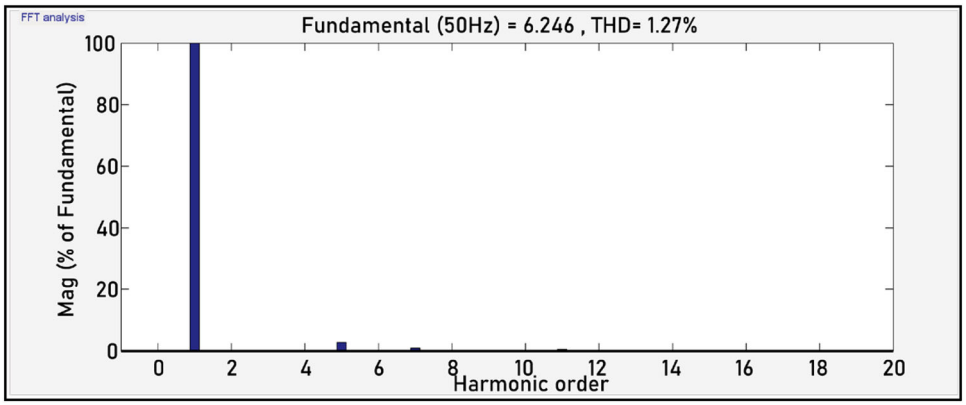

Figure 17. Fourier analysis of source current of load 2 with TS-ANN.

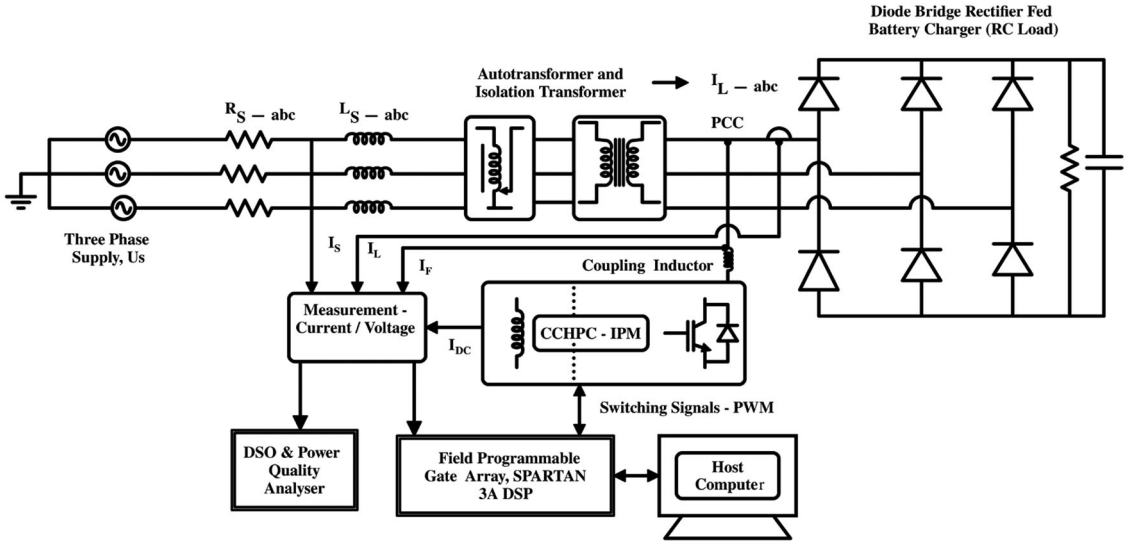

Figure 18. Experimental Setup of the proposed system.

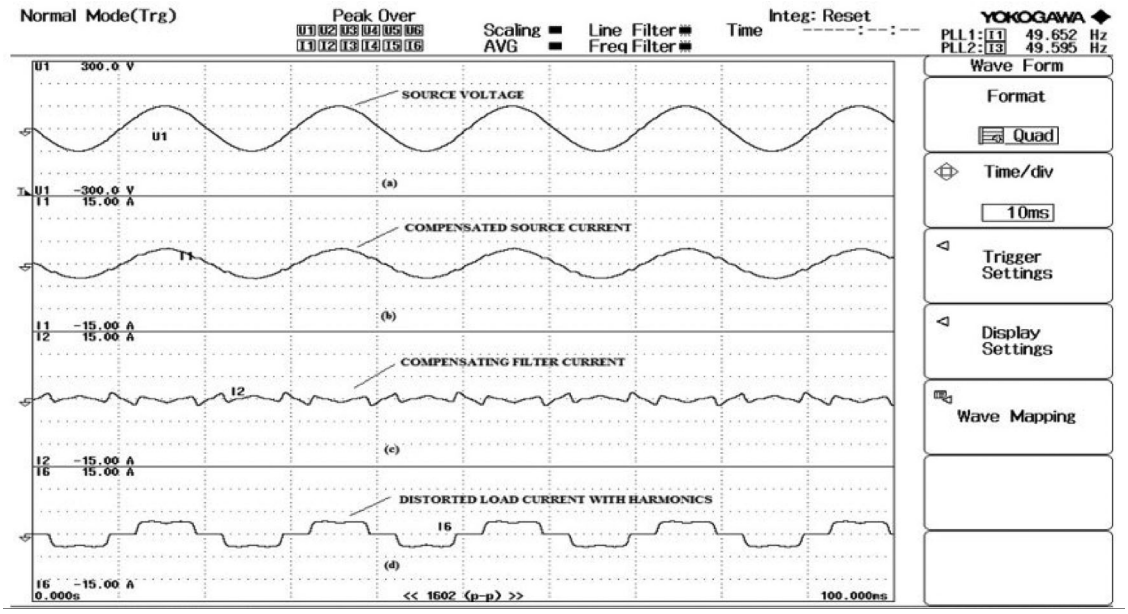

Figure 19. Experimental results: (a) Input source voltage, U_s; (b) Input source current, I_s; (c) Compensated filter current, I_F; (d) Distorted load current, I_L.

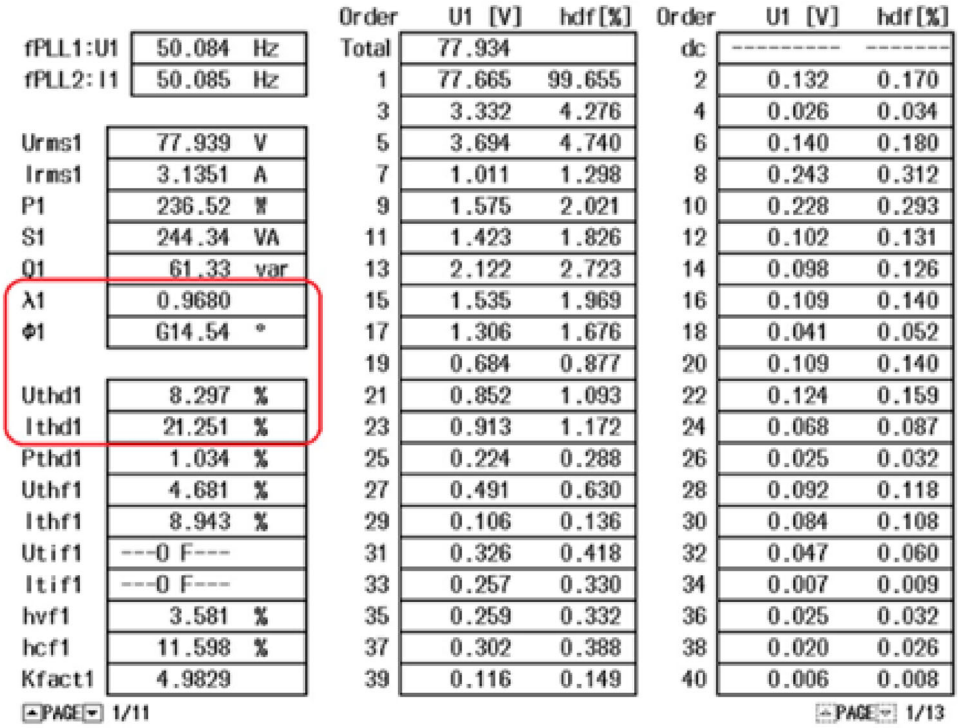

fPLL1:U1	50.084	Hz
fPLL2:I1	50.085	Hz
Urms1	77.939	V
Irms1	3.1351	A
P1	236.52	W
S1	244.34	VA
Q1	61.33	var
λ1	0.9680	
Φ1	G14.54	°
Uthd1	8.297	%
Ithd1	21.251	%
Pthd1	1.034	%
Uthf1	4.681	%
Ithf1	8.943	%
Utif1	---0 F---	
Itif1	---0 F---	
hvf1	3.581	%
hcf1	11.598	%
Kfact1	4.9829	

PAGE 1/11

Order	U1 [V]	hdf[%]	Order	U1 [V]	hdf[%]
Total	77.934		dc	---------	-------
1	77.665	99.655	2	0.132	0.170
3	3.332	4.276	4	0.026	0.034
5	3.694	4.740	6	0.140	0.180
7	1.011	1.298	8	0.243	0.312
9	1.575	2.021	10	0.228	0.293
11	1.423	1.826	12	0.102	0.131
13	2.122	2.723	14	0.098	0.126
15	1.535	1.969	16	0.109	0.140
17	1.306	1.676	18	0.041	0.052
19	0.684	0.877	20	0.109	0.140
21	0.852	1.093	22	0.124	0.159
23	0.913	1.172	24	0.068	0.087
25	0.224	0.288	26	0.025	0.032
27	0.491	0.630	28	0.092	0.118
29	0.106	0.136	30	0.084	0.108
31	0.326	0.418	32	0.047	0.060
33	0.257	0.330	34	0.007	0.009
35	0.259	0.332	36	0.025	0.032
37	0.302	0.388	38	0.020	0.026
39	0.116	0.149	40	0.006	0.008

PAGE 1/13

Figure 20. Experimental results of battery charger with source current before compensation.

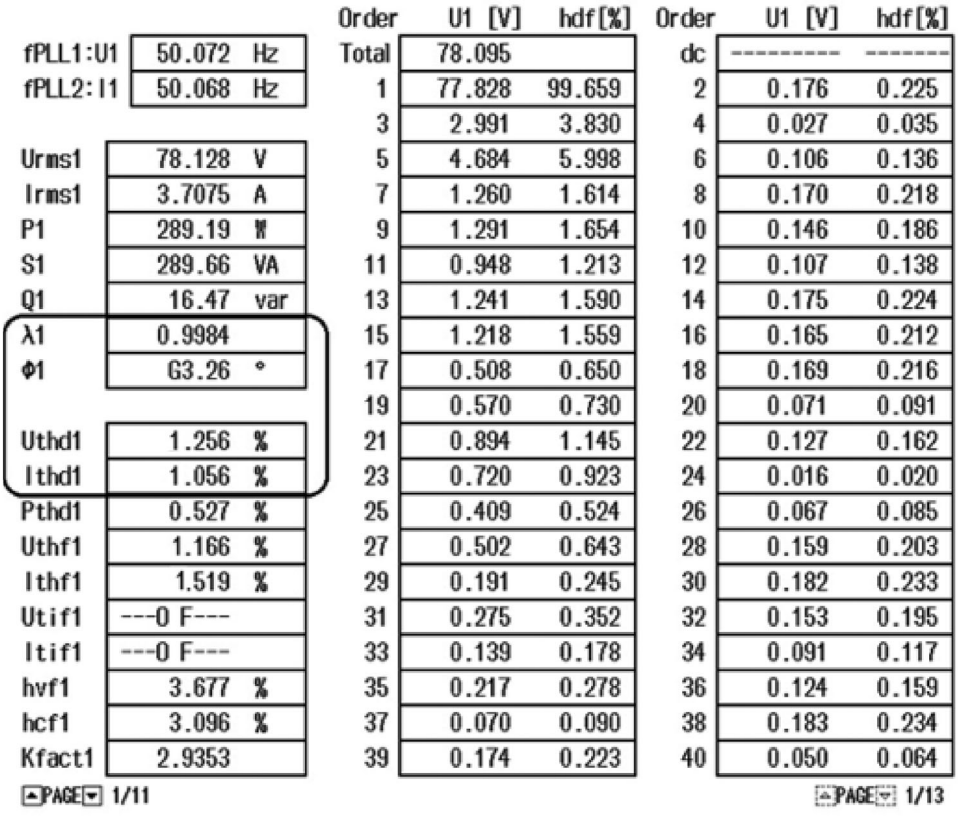

fPLL1:U1	50.072	Hz
fPLL2:I1	50.068	Hz
Urms1	78.128	V
Irms1	3.7075	A
P1	289.19	W
S1	289.66	VA
Q1	16.47	var
λ1	0.9984	
Φ1	G3.26	°
Uthd1	1.256	%
Ithd1	1.056	%
Pthd1	0.527	%
Uthf1	1.166	%
Ithf1	1.519	%
Utif1	---0 F---	
Itif1	---0 F---	
hvf1	3.677	%
hcf1	3.096	%
Kfact1	2.9353	

PAGE 1/11

Order	U1 [V]	hdf[%]	Order	U1 [V]	hdf[%]
Total	78.095		dc	---------	-------
1	77.828	99.659	2	0.176	0.225
3	2.991	3.830	4	0.027	0.035
5	4.684	5.998	6	0.106	0.136
7	1.260	1.614	8	0.170	0.218
9	1.291	1.654	10	0.146	0.186
11	0.948	1.213	12	0.107	0.138
13	1.241	1.590	14	0.175	0.224
15	1.218	1.559	16	0.165	0.212
17	0.508	0.650	18	0.169	0.216
19	0.570	0.730	20	0.071	0.091
21	0.894	1.145	22	0.127	0.162
23	0.720	0.923	24	0.016	0.020
25	0.409	0.524	26	0.067	0.085
27	0.502	0.643	28	0.159	0.203
29	0.191	0.245	30	0.182	0.233
31	0.275	0.352	32	0.153	0.195
33	0.139	0.178	34	0.091	0.117
35	0.217	0.278	36	0.124	0.159
37	0.070	0.090	38	0.183	0.234
39	0.174	0.223	40	0.050	0.064

PAGE 1/13

Figure 21. Experimental results of source current after compensation with TS – ANN.

Source current THD before and after compensation is shown in Figure 20 and 21.

Table 2 compares the experiment results and simulation results of the existing and proposed systems.

5. Conclusions

The development of CC-HAPC is important because it reduces harmonic distortion of input currents, resulting

Table 2. Comparative result of proposed and existing system.

Author name	Technique employed	Performance of source current THD
P. Thirumoorthi et al.	Instantaneous power of PQ theory	
(a) Simulation Results	PI – CSHPF	6.10%
	FLC – CSHPF	4.50%
(b) Experimental Results	FLC-CSHP	2.70%
Manoj Badoni et al.		
(a) Simulation Results	Wiener Filter	1.68%
	Least Mean Square Algorithm	3.00%
(b) Experimental Results	Wiener Filter	2.30%
	Least Mean Square Algorithm	4.10%
N. Narender Reddy et al.	Model Predictive Control Algorithm based Tree structured multi-level Control system Selective Harmonic Elimination Particle Swarm Optimization SHE	
(a) Simulation Results	Improved PSO – SHE	6.31%
	Multitudinal Sliding Mode Control (MSMC)	5.99%
	PI Controller	4.72%
Vijayakumar Gali et al.	Conventional SMC	
	MSMC	
(a) Simulation Results	PI Controller	4.30%
	Conventional SMC	3.84%
	MSMC	1.50%
(b) Experimental Results	Unified Power Quality Conditioner – Nonlinear Sliding Mode Control	4.60%
	Load 1 & Load 2 – Conventional PI controller	3.70%
	Load 1 & Load 2 – UPQC	2.40%
Rajesh Kumar Patjoshi et al.	Neural Learning Algorithm	
	Higher order sliding mode controller and Time series neural network	
	PI tuned HOSMC	
(a) Simulation Results	(Load 1 & Load 2)	3.26% and 4.32%
	TS-ANN tuned HOSMC	
	(Load 1 % Load 2)	2.42% and 2.84%
A. Senthil Kumar et al.	*TS-ANN tuned HOSMC*	2.08%
Raheni T D et al *(Proposed System)*	(Load 1 & Load 2)	
(a) Simulation Results		4.63% and 3.21%
		2.65% and 1.27%
(b) Experimental Results		1.525% and 1.056%

in improved power quality. The current controlled – hybrid power compensator based on a time series neural network is designed to reduce the supply side current harmonics caused by battery chargers. PI and TS-ANN-tuned HOSMC are used to calculate reference current. The performance of CC-HPC with neural algorithm is examined and compared with PI-tuned higher order sliding mode controller. The simulated results are used to validate the control algorithm. The time series neural controller tuned HOSMC has achieved best performance in comparison with classical PI-tuned sliding mode controllers (Table 2). The distortion produced on the supply side is reduced through intelligent control methods.

For battery charging applications, the proposed neural network tuned HOSMC has been effectively validated (Figures 18–21). However, the experimental results demonstrated the viability and efficacy of the HOSMC approach in CC-HAPC. Harmonic distortions are below 5% according to IEEE 519-2014 using time series neural network-based hybrid power compensators. The proposed CC-HPC is most suitable for harmonic mitigation in electrical power distribution systems, especially for medium and high-power applications.

Disclosure statement

No potential conflict of interest was reported by the author(s).

Data availability statement

The data that support the findings of this study are available from the corresponding author, T.D.R., upon reasonable request.

ORCID

Raheni T. D http://orcid.org/0000-0002-9738-5888

References

[1] Kim H-S, Kim J-S. Power quality improvement for grid connected inverters under distorted and unbalanced grids. J Power Electron. 2016;16(4):1578–1586.
[2] Balaji V, Chitra S. Power quality management in electrical rid using SCANN controller-based UPQC. Bullet Polish Acad Sci Techn Sci. 2022;70(1):1–9.
[3] Momeni M, Mazinan AH. Improvement of power quality in grid-connected inverter through adaptation-based control strategy. Energy Ecol Environ. 2019;4(1):37–48.
[4] Phan DH, Huang S. Super-twisting sliding control design of three-phase inverter for stand-alone distributed generation systems. J Control Automat Electric Syst. 2016;27:179–188.
[5] Rajesh Francis P, Shajin H, Uma Sankar L. A novel control scheme for PV/WT/FC/battery to power quality enhancement in micro grid system: a hybrid technique. Energy Sources Part A. 2021, 1–17. DOI:10.1080/15567036.2021.1943068
[6] Gade S, Agrawal R. Optimal utilization of unified power quality conditioner using the JAYA optimization algorithm. Eng Optim. 2021;55:1–18. DOI:10.1080/0305215X.2021.1978440
[7] Gwozdz M, Cieplinski L. An active power filter based on a hybrid converter topology – part 1. Bullet Polish Acad Sci Techn Sci. 2021;69(1):1–10.
[8] Thirumoorthi P, Yadaiah N. Design of current source hybrid power filter for harmonic current compensation. Simul Model Pract Theory. 2015;52:78–91.

[9] Dey P, Mekhilef S. Current controllers of active power filter for power quality improvement: a technical analysis. Automatika. 2015;56(1):42–54.
[10] Badoni M, Singh A, Singh B. Comparative performance of wiener filter and adaptive least mean square-based control for power quality improvement. IEEE Trans Ind Electron. 2016;63(5):3028–3037.
[11] Narender Reddy N, Chandrashekar O, Srujana A. Power quality enhancement by MPC based multilevel control employed with improved particle swarm optimized selective harmonic elimination. Energy Sources Part A. 2019;41(19):2396–2414.
[12] Mohan S, Bhikkaji B, Poongothai C, et al. A linear programming approach for designing multilevel PWM waveforms. Int J Control. 2020;94(9):2584–2595.
[13] Kumaresan S, Habeebullah Sait H. Design and control of shunt active power filter for power quality improvement of utility powered brushless DC motor drives. Automatika. 2020;61(3):507–521.
[14] Thirumoorthi P, Raheni TD. Adaptive method for power quality improvement through minimization of harmonics using artificial intelligence. Int J Power Electron Drive System. 2017;8(1):470–482.
[15] Han Y, Liu X. Continuous higher-order sliding mode control with time-varying gain for a class of uncertain nonlinear systems. ISA Trans. 2016;62:193–201.
[16] Gali V, Gupta N, Gupta RA. Experimental investigations on multitudinal sliding mode controller based interleaved shunt APF to mitigate shoot through and PQ problems under distorted supply voltage conditions. Int Trans Electric Energy Syst. 2018;29(1):1–23.
[17] Alsmadi YM, Utkin V, Haj-ahmed MA, et al. Sliding mode control of power converters: DC/DC converters. Int J Control. 2017;91(11):2472–2493.
[18] Patjoshi RK, Mahapatra K. High-performance unified power quality conditioner using non-linear sliding mode and new switching dynamics control strategy. IET Power Electron. 2017;10(8):863–874.
[19] Kobravia K, Filizadehb S. An adaptive multi-modal optimization algorithm for simulation-based design of power-electronic circuits. Eng Optim. 2009;41(10):945–969.
[20] Senthil Kumar A, Ajay-D-Vimal Raj P. Neural learning algorithm-based power quality enhancement for three phase three wire distribution system utilizing shunt active power filter strategy. In: International Conference on Power and Energy Systems. 2011. IEEE, 1–6. DOI: 10.1109/ICPES.2011.6156667
[21] Iqbal M, Jawad M, Jaffery MH, et al. Neural networks-based shunt hybrid active power filter for harmonic elimination. IEEE Access. 2021;9:69913–69925.

Appendix 1: Design of passive power compensator for fifth order harmonic

(a) $V_S = 440$ V; $F = 50$ Hz; $\alpha = 30^\circ$
$V_{S1} = \frac{440}{\sqrt{3}} = 254.03$ V
(b) AC load RMS current, $I_L = \frac{I_{DC}\sqrt{2}}{\sqrt{3}}$
DC link inductor current is 1.85 A (measured); $I_L = 1.5103$ A
(c) Fundamental RMS value of load current (I_{L1}) is calculated as,
$I_{L1} = \left(\frac{\sqrt{6}}{\pi}\right) I_L$; Therefore $I_{L1} = 1.17757$ A
(d) The load current active component is determined by,
$I_{La} = I_{L1} \cos 30^\circ = 1.01980$ A
(e) Active power is calculated by the following equation,
$P_1 = 3V_{S1}I_{L1} \cos 30^\circ = 1171.942$ W
(f) Reactive power is computed as follows,
$Q_1 = 3V_{S1}I_{L1} \sin 30^\circ = 676.621$ VAR
(g) Filter capacitor, C_F

$$C_F = \frac{Q_1}{m\omega V_S^2}$$

m – Number of phases
ω – Fundamental frequency of the supply
$C_F = 0.7411$ μF
(h) Filter inductor, L_F
$L_F = \frac{1}{\omega^2 C_F} = L_F = 546.859$ mH

Appendix 2: MATLAB coding for neural network

```
% Solve an Input-Output Time-Series Problem with a Time Delay Neural Network
% Script generated by NTSTOOL.
% Created Wed May 16 9:59:30 IST 2022
%
% This script assumes these variables are defined:
%
% data - input time series.
% data - target time series.
inputSeries = tonndata(data,false,false);
targetSeries = tonndata(data,false,false);
% Create a Time Delay Network
inputDelays = 1:2;
hiddenLayerSize = 30;
net = timedelaynet(inputDelays,hiddenLayerSize);
% Choose Input and Output Pre/Post-Processing Functions
% For a list of all processing functions type: help nnprocess
net.inputs1.processFcns = 'removeconstantrows', 'mapminmax';
net.outputs2.processFcns = 'removeconstantrows', 'mapminmax';
% Prepare the Data for Training and Simulation
% The function PREPARETS prepares timeseries data for a particular network,
% shifting time by the minimum amount to fill input states and layer states.
% Using PREPARETS allows you to keep your original time series data unchanged, while
% easily customizing it for networks with differing numbers of delays, with
% open loop or closed loop feedback modes.
[inputs,inputStates,layerStates,targets] = preparets(net,inputSeries,targetSeries);
% Setup Division of Data for Training, Validation, Testing
% For a list of all data division functions type: help nndivide
net.divideFcn = 'dividerand'; % Divide data randomly
net.divideMode = 'time'; % Divide up every value
net.divideParam.trainRatio = 70/100;
net.divideParam.valRatio = 15/100;
net.divideParam.testRatio = 15/100;
% For help on training function 'trainlm' type: help trainlm
% For a list of all training functions type: help nntrain
net.trainFcn = 'trainlm'; % Levenberg-Marquardt
% Choose a Performance Function
% For a list of all performance functions type: help nnperformance
net.performFcn = 'mse'; % Mean squared error
% Choose Plot Functions
% For a list of all plot functions type: help nnplot
```

```
net.plotFcns = 'plotperform','plottrainstate','plotresponse',
...
'ploterrcorr', 'plotinerrcorr';
% Train the Network
[net,tr] = train(net,inputs,targets,inputStates,layerStates);
% Test the Network
outputs = net(inputs,inputStates,layerStates);
errors = gsubtract(targets,outputs);
performance = perform(net,targets,outputs)
% Recalculate Training, Validation and Test Performance
trainTargets = gmultiply(targets,tr.trainMask);
valTargets = gmultiply(targets,tr.valMask);
testTargets = gmultiply(targets,tr.testMask);
trainPerformance = perform(net,trainTargets,outputs)
valPerformance = perform(net,valTargets,outputs)
testPerformance = perform(net,testTargets,outputs)
% View the Network
view(net)
% Plots
% Uncomment these lines to enable various plots.
%figure, plotperform(tr)
%figure, plottrainstate(tr)
%figure, plotresponse(targets,outputs)
%figure, ploterrcorr(errors)
%figure, plotinerrcorr(inputs,errors)
% Early Prediction Network
% For some applications it helps to get the prediction a
timestep early.
% The original network returns predicted y(t+1) at the same
time it is given x(t+1).
% For some applications such as decision making, it would
help to have predicted
% y(t+1) once x(t) is available, but before the actual y(t+1)
occurs.
% The network can be made to return its output a timestep
early by removing one delay
% so that its minimal tap delay is now 0 instead of 1. The new
network returns the
% same outputs as the original network, but outputs are
shifted left one timestep.
nets = removedelay(net);
[xs,xis,ais,ts] = preparets(nets,inputSeries,targetSeries);
ys = nets(xs,xis,ais);
earlyPredictPerformance = perform(net,ts,ys)
```